

Topological susceptibility at zero and finite temperature in the Nambu–Jona-Lasinio model

K. Fukushima*, K. Ohnishi†, and K. Ohta‡

Institute of Physics, University of Tokyo, 3-8-1 Komaba, Meguro-ku, Tokyo 153-8902, Japan

Abstract

We consider the three flavor Nambu–Jona-Lasinio model with the 't Hooft interaction incorporating the $U(1)_A$ anomaly. In order to set the coupling strength of the 't Hooft term, we employ the topological susceptibility χ instead of the η' meson mass. The value for χ is taken from lattice simulations. We also calculate χ at finite temperature within the model. Comparing it with the lattice data, we extract information about the behavior of the $U(1)_A$ anomaly at finite temperature. We conclude that within the present framework, the effective restoration of the $U(1)_A$ symmetry does not necessarily take place even at high temperature where the chiral symmetry is restored.

11.30.Rd, 12.39.Fe

Typeset using REVTeX

*E-mail: fuku@nt1.c.u-tokyo.ac.jp

†E-mail: konishi@nt1.c.u-tokyo.ac.jp

‡E-mail: ohta@nt1.c.u-tokyo.ac.jp

I. INTRODUCTION

The $U(1)_A$ anomaly of QCD plays an essential role in hadron physics. One of its most striking manifestations would probably be the η' meson mass. Since the $U(1)_A$ symmetry is broken not spontaneously but explicitly by the anomaly, η' cannot be regarded as a nearly massless Nambu-Goldstone boson like the other pseudoscalar mesons. In fact, the mass of η' is as large as the nucleon mass, i.e. $m_{\eta'} = 958$ MeV. This is the so-called $U(1)_A$ problem.

The topological susceptibility, χ , is an essential quantity in considering the $U(1)_A$ problem because it is related to $m_{\eta'}$ through the Witten-Veneziano mass formula [1,2],

$$\frac{2N_f}{f_\pi^2}\chi = m_\eta^2 + m_{\eta'}^2 - 2m_K^2, \quad (1)$$

where $N_f = 3$ is the number of the flavors and f_π is the pion decay constant. This formula has been confirmed by calculating χ directly on the lattice [7]: The calculations give $\chi \sim (180 \text{ MeV})^4$, which is consistent with the value obtained by plunging into the formula (1) experimental values of the pion decay constant and the meson masses. Thus, the topological susceptibility could tell us as much information about the $U(1)_A$ anomaly as does $m_{\eta'}$.

The tool we will employ in this work for the investigation of the $U(1)_A$ problem is the three flavor Nambu–Jona-Lasinio (NJL) model [3–6] which can be used as an effective theory of QCD. The NJL Lagrangian we adopt here is

$$\mathcal{L} = \mathcal{L}_0 + \mathcal{L}_4 + \mathcal{L}_6, \quad (2)$$

$$\mathcal{L}_0 = \bar{q}(i\gamma_\mu\partial^\mu - m)q, \quad (3)$$

$$\mathcal{L}_4 = G \sum_{a=0}^8 [(\bar{q}\lambda^a q)^2 + (\bar{q}i\gamma_5\lambda^a q)^2], \quad (4)$$

$$\mathcal{L}_6 = -K [\det \bar{q}(1 + \gamma_5)q + \det \bar{q}(1 - \gamma_5)q], \quad (5)$$

where the quark field q is a column vector in the color, flavor and spinor spaces, and λ^a is the Gell-Mann matrix in the flavor space with $\lambda^0 = \sqrt{2/3} \text{diag}(1, 1, 1)$. The determinants in Eq. (5) are with respect to the flavor indices.

The free quark Lagrangian \mathcal{L}_0 contains the current quark mass term with $m = \text{diag}(m_u, m_d, m_s)$, breaking the $U(3)_L \otimes U(3)_R$ symmetry explicitly. Throughout this article, we assume the exact isospin symmetry, i.e. $m_u = m_d$. The term \mathcal{L}_4 generates the four-point couplings and is invariant under the $U(3)_L \otimes U(3)_R$ transformation. The six-point, determinant term \mathcal{L}_6 is what is called the 't Hooft interaction and breaks the $U(1)_A$ symmetry. This interaction simulates the $U(1)_A$ anomaly in our scheme, and the effective coupling constant K measures its strength.

Let us review the status of parameter setting in the NJL model. The parameters to be fixed are, the current quark masses ($m_u = m_d, m_s$), the three-momentum cut-off (Λ), and the effective coupling constants (G and K). The physical quantities usually taken as inputs are, m_π , f_π , m_K , and $m_{\eta'}$. The question we bring out here is as to $m_{\eta'}$ which has been used for the determination of K . As is well known, the NJL model lacks in confinement, and in fact, in this model η' decays into asymptotic $q\bar{q}$ states due to its large mass. Thus $m_{\eta'}$ in the NJL model is not a well-defined quantity. The alternative quantity for the determination of K we will use here is the topological susceptibility, which contains the information about the $U(1)_A$ anomaly and whose value has been given by lattice Monte-Carlo simulations, as mentioned above. One of the main purposes in the current work is to derive the expression for the topological susceptibility within the framework of the NJL model, and to fix the parameter K by means of χ as an input.

Recently, the behavior of the effect of the $U(1)_A$ anomaly at finite temperature has been discussed intensively [9,11–14]. In particular, special attentions have been paid to whether or not the effective restoration of the $U(1)_A$ symmetry and the chiral phase transition occur simultaneously. This question is still controversial and is not settled yet. Here, we should clarify what we mean by ‘the effective restoration of the $U(1)_A$ symmetry.’ It means that all $U(1)_A$ violating quantities vanish, i.e. that all order parameters of the $U(1)_A$ symmetry

vanish.¹ The possibility that η' would degenerate with the other pseudoscalar mesons has a great deal of significance upon the experimental view in relativistic heavy ion collisions [10]. In the NJL model, the definition we gave above is equivalent to K getting to zero, since finite K makes the $U(1)_A$ symmetry breaking manifest in the NJL lagrangian (2). Since the origin from which a finite value of K arises is the presence of instantons in the physical state, the effective restoration of the $U(1)_A$ symmetry is expected owing to the naive argument that the instanton density will be suppressed at sufficiently high temperature. Thus when the magnitude of K becomes smaller, we will call it ‘the effective restoration of the $U(1)_A$ symmetry.’

The temperature dependence of K in the NJL model, which indicates nothing but the temperature dependence of the $U(1)_A$ anomaly, has been put by hand and not gone beyond phenomenology [4]. This is both because experimental data for $m_{\eta'}$ at finite temperature, which are necessary for determination of K , are not available, and because η' becomes unbound completely in the model soon after we raise the temperature from zero. Since the topological susceptibility has been calculated at finite temperature on the lattice, we will be able to determine the temperature dependence of K using that data, and obtain some knowledge about the effective restoration of the $U(1)_A$ symmetry.

The paper is organized as follows. In Sec. II, we will derive the expression for χ in the NJL model. Sec. III is devoted to parameter setting of the model and numerical calculations of the physical quantities. A summary is given in Sec. IV.

II. TOPOLOGICAL SUSCEPTIBILITY IN THE NJL MODEL

In this section, we calculate the topological susceptibility, χ , within the framework of the NJL model.

¹The authors thank the unknown referee for his suggestion on the definite meaning of the $U(1)_A$ symmetry restoration.

The first task is to know a general expression of χ . We recapitulate here the definition of χ . We begin with the QCD Lagrangian density

$$\mathcal{L}_{\text{QCD}} = -\frac{1}{4}F_{\mu\nu}^a F^{a\mu\nu} + \bar{q}(i\gamma_\mu D^\mu - m)q + \theta Q, \quad (6)$$

where $F_{\mu\nu}^a$ is the gluon field strength tensor, $D_\mu = \partial_\mu + igA_\mu$ is the covariant derivative with A_μ being the gluon field, θ is the QCD vacuum angle, and Q is the topological charge density defined by

$$Q(x) = \frac{g^2}{32\pi^2} F_{\mu\nu}^a \tilde{F}^{a\mu\nu}. \quad (7)$$

With this Lagrangian density, the vacuum energy density ε is written as

$$e^{-\varepsilon VT} = \int \mathcal{D}A_\mu \mathcal{D}\bar{q} \mathcal{D}q e^{\int d^4x \mathcal{L}_{\text{QCD}}} \equiv Z \quad (8)$$

in a path integral form, where V and T are the space and time volumes, respectively. The topological susceptibility χ is defined as a second derivative of ε with respect to θ at $\theta = 0$,

$$\chi \equiv \left. \frac{\partial^2 \varepsilon}{\partial \theta^2} \right|_{\theta=0} = \int d^4x \langle 0 | T Q(x) Q(0) | 0 \rangle_{\text{connected}}, \quad (9)$$

where T stands for the time ordering operator, and the subscript ‘connected’ means to pick out the diagrammatically connected contributions. Thus, in order to calculate χ in the NJL model, it is necessary to find a correspondent to $Q(x)$ in the model. For that purpose, we consider the four-divergence of the $U(1)_A$ current, $J_{5\mu} = \bar{q}\gamma_\mu\gamma_5q$. In QCD, one has

$$\partial^\mu J_{5\mu} = 2N_f Q(x) + 2i\bar{q}m\gamma_5q, \quad (10)$$

which does not vanish due to the anomaly.

On the other hand, in the NJL model (Eqs. (2)~(5)), we find [4]

$$\partial^\mu J_{5\mu} = 4N_f K \text{Im det } \Phi + 2i\bar{q}m\gamma_5q, \quad (11)$$

where

$$\Phi_{ij} = \bar{q}_i(1 - \gamma_5)q_j, \quad (12)$$

and i, j denote the flavor indices. Comparing these two expressions, we find that

$$\begin{aligned} Q(x) &= 2K \text{Im} \det \Phi \\ &= -iK [\det \Phi - (\det \Phi)^*] \end{aligned} \quad (13)$$

in the NJL model.

With the definition of $\Gamma_{\pm} \equiv 1 \pm \gamma_5$, we can write

$$\begin{aligned} \det \Phi &= \frac{1}{3!} \epsilon^{abc} \epsilon^{ijk} (\bar{q}_i \Gamma_{-q_a})(\bar{q}_j \Gamma_{-q_b})(\bar{q}_k \Gamma_{-q_c}), \\ (\det \Phi)^* &= \frac{1}{3!} \epsilon^{def} \epsilon^{lmn} (\bar{q}_l \Gamma_{+q_d})(\bar{q}_m \Gamma_{+q_e})(\bar{q}_n \Gamma_{+q_f}) \end{aligned} \quad (14)$$

so that

$$\begin{aligned} \chi &= \int d^4x \langle 0 | T Q(x) Q(0) | 0 \rangle_{\text{connected}} \\ &= -\frac{K^2}{(3!)^2} \int d^4x \epsilon^{abc} \epsilon^{ijk} \epsilon^{def} \epsilon^{lmn} \\ &\times \langle 0 | T \{ (\bar{q}_i \Gamma_{-q_a})(\bar{q}_j \Gamma_{-q_b})(\bar{q}_k \Gamma_{-q_c})(x)(\bar{q}_l \Gamma_{-q_d})(\bar{q}_m \Gamma_{-q_e})(\bar{q}_n \Gamma_{-q_f})(0) \\ &\quad - (\bar{q}_i \Gamma_{-q_a})(\bar{q}_j \Gamma_{-q_b})(\bar{q}_k \Gamma_{-q_c})(x)(\bar{q}_l \Gamma_{+q_d})(\bar{q}_m \Gamma_{+q_e})(\bar{q}_n \Gamma_{+q_f})(0) \\ &\quad - (\bar{q}_i \Gamma_{+q_a})(\bar{q}_j \Gamma_{+q_b})(\bar{q}_k \Gamma_{+q_c})(x)(\bar{q}_l \Gamma_{-q_d})(\bar{q}_m \Gamma_{-q_e})(\bar{q}_n \Gamma_{-q_f})(0) \\ &\quad + (\bar{q}_i \Gamma_{+q_a})(\bar{q}_j \Gamma_{+q_b})(\bar{q}_k \Gamma_{+q_c})(x)(\bar{q}_l \Gamma_{+q_d})(\bar{q}_m \Gamma_{+q_e})(\bar{q}_n \Gamma_{+q_f})(0) \} | 0 \rangle_{\text{connected}}. \end{aligned} \quad (15)$$

Now we must evaluate these four matrix elements. For the time being, we pick up one term out of the four. Following Wick's theorem, we take full contraction in terms of the propagator $S(x, x')$ that has been constructed in the self-consistent gap equation [3–6]. Although several ways of contraction are possible, there exists only one that is the leading order in expansion in terms of inverse powers of the number of colors, i.e. $1/N_c$. The situation is demonstrated in Fig. 1 by means of the finite range representation.

The diagrams (a) and (b) in Fig. 1 contain N_c^4 coming from traces over color. The diagram (c) contains N_c^5 and is the leading order in $1/N_c$ expansion. Notice that (b) is the exchange term for (c) and is lowered by $1/N_c$ as compared with (c). Since the gap equation for the constituent quark masses and the dispersion equations for the meson masses are

derived up to the leading order of the large N_c expansion [3], we should take only the contribution of (c) for the consistent treatment.

Taking account of the four terms in Eq. (15), we obtain the following expression for the lowest order of the diagrammatical expansion,

$$\begin{aligned} \chi^{(\text{lowest})} = & -\frac{K^2}{(3!)^2} (-9) \epsilon^{abc} \epsilon^{ijk} \epsilon^{def} \epsilon^{lmn} 4 \left\{ \int d^4x N_c \text{tr} [S_{di}(x) \gamma_5 S_{al}(x) \gamma_5] \right\} \\ & \times N_c^4 \text{tr} [S_{bj}(0)] \text{tr} [S_{ck}(0)] \text{tr} [S_{em}(0)] \text{tr} [S_{fn}(0)], \end{aligned} \quad (16)$$

where the full propagator in the Euclidean space is given as

$$S_{ij}(x) = \delta_{ij} \int \frac{d^4p}{(2\pi)^4} \frac{\not{p} + m_i^*}{-p^2 - m_i^{*2}} e^{-ip \cdot x}, \quad (17)$$

and m_i^* denotes the constituent quark mass.

The object in the curly brackets in Eq. (16) corresponds to the one-loop part connecting the points x and 0 in Fig. 1(c). This is basically the one-loop proper polarization insertion $\Pi_{ij}^{\text{ps}}(k^2)$ [3–6] with $k^2 = 0$ although the trace over flavor is not taken in this case. Especially in the case of $a = i$ and $d = l$, which is the condition for giving non-zero contribution to $\chi^{(\text{lowest})}$ due to the ε -tensor in Eq. (16), the object can be identified with an element of 3-, 8-, 0-channel polarizations with $k^2 = 0$; for instance, 0-0 channel polarization is

$$\begin{aligned} \Pi_{00}^{\text{ps}}(k^2 = 0) = & \text{tr}_{\text{flavor}} \frac{2}{3} \text{diag} \left(-N_c \int \frac{d^4p}{(2\pi)^4} \text{tr} [i\gamma_5 S^u(p) i\gamma_5 S^u(p)], \right. \\ & \left. -N_c \int \frac{d^4p}{(2\pi)^4} \text{tr} [i\gamma_5 S^d(p) i\gamma_5 S^d(p)], -N_c \int \frac{d^4p}{(2\pi)^4} \text{tr} [i\gamma_5 S^s(p) i\gamma_5 S^s(p)] \right). \end{aligned} \quad (18)$$

Actually, there exist other diagrams that are of the same order in $1/N_c$ expansion as the diagram in Fig. 1(c). They are shown in Fig. 2. They are of the same order as Fig. 1(c) because, while each four-point vertex is of $O(N_c^{-1})$ [3], it is compensated by a factor N_c coming from its neighboring loop. We have to include all these diagrams for consistency of the $1/N_c$ expansion. We will call their sum $\chi^{(\text{ring})}$, for they are regarded as the ring diagrams to be resummed in the mean field approximation.

Of course, the sum of these ring diagrams with the one-loop diagram included can be interpreted as a propagation of a certain meson. Note that the momentum of the propagating

particle is zero; $k^2 = 0$. This is just the reflection of the fact that χ is the quantity of the zero frequency mode of the Fourier transform of $\langle TQ(x)Q(0) \rangle$, namely,

$$\chi = \int d^4x e^{-ik \cdot x} \langle TQ(x)Q(0) \rangle \Big|_{k=0}. \quad (19)$$

Now we calculate $\chi^{(\text{ring})}$ following the Feynman rules of the NJL Lagrangian. We note that the diagrams in Fig. 2 are obtained by replacing the one-loop polarization part in Fig. 1(c) with the ring diagrams. Correspondingly we can obtain $\chi^{(\text{ring})}$ by replacing the curly bracketed part in Eq. (16) with the sum of the ring diagrams. We first perform the summation over flavor indices. After that, it can be shown that the expressions corresponding to each edge point of a diagram in Fig. 2 are brought together into a matrix form and are arranged to the linear combination of λ_8 and λ_0 matrices. In other words, the 8- and 0-channel vertices have been assigned to each edge point of each ring diagram in Fig. 2. Then following the Feynman rules, we can construct the ring diagrams by linking 8-, 0-channel polarizations $\Pi_{88}^{\text{ps}}(k^2=0)$, $\Pi_{80}^{\text{ps}}(k^2=0) = \Pi_{08}^{\text{ps}}(k^2=0)$, $\Pi_{00}^{\text{ps}}(k^2=0)$, and 8-, 0-channel vertices $K_{88}^{(+)}$, $K_{80}^{(+)} = K_{08}^{(+)}$, $K_{00}^{(+)}$, in all possible ways. The result is

$$\begin{aligned} \chi^{(\text{ring})} = & 4N_c^4 K^2 \left\{ \frac{1}{\sqrt{3}} \text{tr} S^u (\text{tr} S^s - \text{tr} S^u) \begin{pmatrix} \Pi_{88} \\ \Pi_{80} \end{pmatrix}^t + \frac{1}{\sqrt{6}} \text{tr} S^u (2\text{tr} S^s + \text{tr} S^u) \begin{pmatrix} \Pi_{08} \\ \Pi_{00} \end{pmatrix}^t \right\} \\ & \times 2\hat{K} (1 - 2\hat{\Pi}\hat{K})^{-1} \\ & \times \left\{ \frac{1}{\sqrt{3}} \text{tr} S^u (\text{tr} S^s - \text{tr} S^u) \begin{pmatrix} \Pi_{88} \\ \Pi_{08} \end{pmatrix} + \frac{1}{\sqrt{6}} \text{tr} S^u (2\text{tr} S^s + \text{tr} S^u) \begin{pmatrix} \Pi_{80} \\ \Pi_{00} \end{pmatrix} \right\}, \quad (20) \end{aligned}$$

where

$$\hat{K} = \begin{pmatrix} K_{88}^{(+)} & K_{80}^{(+)} \\ K_{08}^{(+)} & K_{00}^{(+)} \end{pmatrix}, \quad \hat{\Pi} = \begin{pmatrix} \Pi_{88} & \Pi_{80} \\ \Pi_{08} & \Pi_{00} \end{pmatrix} \quad (21)$$

are 2×2 matrices, and

$$\Pi_{ij} = \Pi_{ij}^{\text{ps}}(k^2=0), \quad \text{tr} S^i = \text{tr} S^i(x=0). \quad (22)$$

For example, the first term in the first curly brackets of Eq. (20) produces contributions from the diagrams whose one edge point is an 8-channel vertex. And, again for example,

the second term in the second curly brackets of Eq. (20) produces contributions from the diagrams the other edge point of which is a 0-channel vertex. The 8-8 and 0-0 channel diagrams can be interpreted as the propagations of η_8 and η_0 mesons respectively. We see that in addition to the η_8 and η_0 propagations, there occur 8-0 and 0-8 mixing channel diagrams.

Another comment is in order. If $\text{tr}S^u = \text{tr}S^s$, that is, the $SU(3)_V$ symmetry is exact, the 8-channel vertices in Eq. (20) vanish. In this case, 8- and mixing channel polarizations Π_{88}^{ps} , $\Pi_{80}^{\text{ps}} = \Pi_{08}^{\text{ps}}$ as well as 8- and mixing channel vertices $K_{88}^{(+)}$, $K_{80}^{(+)} = K_{08}^{(+)}$ all vanish, so that only the ring diagrams constructed by those of the 0-channel, Π_{00}^{ps} and $K_{00}^{(+)}$, contribute to $\chi^{(\text{ring})}$, which are interpreted as the propagation of the pure η_0 state.

Finally, combining Eqs. (16) and (20), we arrive at the expression for the topological susceptibility,

$$\begin{aligned} \chi = 4N_c^4 K^2 & \left[-N_c (\text{tr}S^u)^4 (\text{tr}S^s)^2 \left(\frac{2}{m_u^* \text{tr}S^u} + \frac{1}{m_s^* \text{tr}S^s} \right) \right. \\ & + \left\{ \frac{1}{\sqrt{3}} \text{tr}S^u (\text{tr}S^s - \text{tr}S^u) \begin{pmatrix} \Pi_{88} \\ \Pi_{80} \end{pmatrix}^t + \frac{1}{\sqrt{6}} \text{tr}S^u (2\text{tr}S^s + \text{tr}S^u) \begin{pmatrix} \Pi_{08} \\ \Pi_{00} \end{pmatrix}^t \right\} \\ & \times 2\hat{K} (1 - 2\hat{\Pi}\hat{K})^{-1} \\ & \left. \times \left\{ \frac{1}{\sqrt{3}} \text{tr}S^u (\text{tr}S^s - \text{tr}S^u) \begin{pmatrix} \Pi_{88} \\ \Pi_{08} \end{pmatrix} + \frac{1}{\sqrt{6}} \text{tr}S^u (2\text{tr}S^s + \text{tr}S^u) \begin{pmatrix} \Pi_{80} \\ \Pi_{00} \end{pmatrix} \right\} \right]. \quad (23) \end{aligned}$$

Let us give one more comment. In general, a two-point correlation function of gauge invariant operators may be decomposed into the sum over multi-particle intermediate states by inserting a complete set between two operators. It is known that the dominant contributions of the leading order in $1/N_c$ expansion are those of one-particle intermediate states. Moreover Witten [1] and Veneziano [2] have derived their formula by assuming that, when the momentum of the intermediate particle is zero, which is the case of χ , the contribution of the η_0 propagating state is the only leading term in $1/N_c$ expansion. These statements are quite consistent with our specific model calculation respecting large N_c expansion (although η_8 and mixing channels besides η_0 propagate in the intermediate states in our model due to the explicit $SU(3)_V$ symmetry breaking).

III. NUMERICAL CALCULATION

Now that we have obtained the expression for the topological susceptibility, we proceed to numerical calculations. In Sec. III A, we set the parameters at zero temperature by employing χ . With the determined parameters, we calculate physical quantities. In Sec. III B, we discuss the temperature dependence of χ and the six-point coupling constant K .

A. Parameter setting at zero temperature

The parameters to be set in the NJL model are;

$$\left\{ \begin{array}{ll} \text{current quark masses} & m_u = m_d, \quad m_s \\ \text{three-momentum cut-off} & \Lambda \\ \text{four-point coupling constant} & G \\ \text{six-point coupling constant} & K. \end{array} \right.$$

As for $m_u = m_d$, we set them to be $m_u = m_d = 5.5$ MeV following Ref. [4].

To set the other four parameters, we use the following quantities as inputs,

$$\left\{ \begin{array}{ll} m_\pi & = \quad 138 \text{ MeV} \\ f_\pi & = \quad 93 \text{ MeV} \\ m_K & = \quad 495.7 \text{ MeV} \\ \chi & = (175 \pm 5 \text{ MeV})^4. \end{array} \right.$$

The fourth quantity we use here in place of $m_{\eta'} = 957.5$ MeV is, as mentioned in the introduction, the topological susceptibility χ . The numerical value of χ is taken from Ref. [7], in which χ is calculated in the quenched approximation.

Initially, however, we will calculate with the parameters determined by using $m_{\eta'}$ as input in order to check consistency of $m_{\eta'}$ and χ in the NJL model. Parameter setting with $m_{\eta'}$ has been performed in Ref. [4], and the results are

$$m_s = 135.7 \text{ MeV}, \quad \Lambda = 631.4 \text{ MeV}, \quad G\Lambda^2 = 1.835, \quad K\Lambda^5 = 9.29.$$

The physical quantities calculated from these parameters are summarized in the first column of Table I. We first check the Witten-Veneziano mass formula (1) within the NJL model.

The computed values of χ and m_η with those parameters of Ref. [4] are

$$\begin{cases} \chi_{\text{NJL}} = (166 \text{ MeV})^4 \\ m_\eta = 487 \text{ MeV}, \end{cases}$$

so that the ratio of LHS to RHS in Eq. (1) turns out to be

$$\frac{2N_f\chi}{f_\pi^2(m_\eta^2 + m_{\eta'}^2 - 2m_K^2)} = 0.81. \quad (24)$$

On the other hand, the ratio of χ_{NJL} to χ_{Lat} , which means how much the conventional parameters determined with $m_{\eta'}$ reproduces the lattice data of χ , is

$$\frac{\chi_{\text{NJL}}}{\chi_{\text{Lat}}} = 0.80. \quad (25)$$

From the above two ratios, we can say that as a whole, $m_{\eta'}$ and χ are reproduced well simultaneously in the NJL model.

Now we consider parameter setting with χ used. The topological susceptibility, χ might be a more suitable quantity for parameter setting than $m_{\eta'}$ for the following two reasons:

- Since η' decays into asymptotic $q\bar{q}$ state due to lack of confinement in the NJL model, $m_{\eta'}$ may be a less reliable quantity, while χ is free from such a shortcoming of the NJL model.
- The value of χ , $(175 \text{ MeV})^4$ is small enough compared with the cut-off $\Lambda \sim 600 \text{ MeV}$. Thus the NJL model is expected to describe χ well.

The parameters obtained by using $\chi = (175 \text{ MeV})^4$ are

$$m_s = 135.7 \text{ MeV}, \quad \Lambda = 631.4 \text{ MeV}, \quad G\Lambda^2 = 1.765, \quad K\Lambda^5 = 11.32.$$

We note that $K\Lambda^5$ becomes larger than the case of using $m_{\eta'}$ as an input, which implies that the binding of η' is loosened. (The 't Hooft interaction loosens the binding of mesons,

that is, induces a repulsive force between quarks. This can be seen from the very fact that η' becomes massive due to the interaction.) Physical quantities calculated with these parameters are shown in the second column of Table I. The solution for $m_{\eta'}$ in the mean field approach does not exist, that is, η' is not bound any more. We see that m_η is improved slightly. Although η' no longer exists in the NJL model, we could infer its mass by utilizing the Witten-Veneziano mass formula (1); $m_{\eta'} = 942$ MeV is obtained.

We close this subsection by referring to the study due to Takizawa, Nemoto, and Oka [8], in which the parameters, especially the six-point coupling constant K , are determined in a different approach. They examined the radiative decays of an η meson such as $\eta \rightarrow 2\gamma$, $\eta \rightarrow \gamma l^- l^+$ and $\eta \rightarrow \pi^0 \gamma \gamma$, and obtained rather strong six-point coupling constant $K\Lambda^5$, namely, four times as large as that determined by using $m_{\eta'}$. Although we cannot compare our parameters directly with theirs due to different cut-off schemes (their scheme is the four-momentum cut-off), it is not probable that our result is compatible with theirs. Still, we believe that our approach is rather straightforward to probe the $U(1)_A$ anomaly.

B. Behavior of K at finite temperature

In this subsection, we discuss the temperature dependence of K , comparing the NJL calculation of χ with the lattice data.

The lattice data for the topological susceptibility [7] are shown in Fig. 3 with error bars. The T_c in the figure denotes the temperature of the chiral phase transition. Although $T_c = 260$ MeV in the original Ref. [7], we have rescaled it to 150 MeV. We should notice that the lattice data are computed only up to $T = 1.4T_c$. Unfortunately, the lattice data are absent at high temperatures. At any rate, the data show that χ drops rapidly around T_c .

One comment should be noted. The fact that χ drops near T_c does not always mean the effective restoration of the $U(1)_A$ symmetry at T_c . This can be seen by returning to the Witten-Veneziano mass formula (1),

$$2N_f \chi = f_\pi^2 (m_\eta^2 + m_{\eta'}^2 - 2m_K^2). \quad (1')$$

We realize that the pion decay constant f_π , which is associated with the spontaneous chiral symmetry breaking ($SU(3)_L \otimes SU(3)_R \rightarrow SU(3)_V$), has entered the formula. Since f_π would become zero along with the restoration of the chiral symmetry, χ is also expected to become zero around T_c . In this sense, the lattice data which show the dropping of χ at T_c is what should be expected from the formula, and rather, we could consider that the data confirm the validity of the Witten-Veneziano mass formula. Thus the dropping of χ in the lattice data should be attributed to the restoration of the chiral symmetry, and does not always indicate the effective restoration of the $U(1)_A$ symmetry. It is worth noting that this behavior results from large N_c expansion. In Ref. [16] it was pointed out that n -point correlation functions ($n < N_f = 3$) cannot detect any effect of the $U(1)_A$ anomaly in the chiral symmetric phase. One might have thought that the dropping of χ near T_c would be regarded as χ 's insensitivity to the $U(1)_A$ anomaly. However, it is not the case because χ is not a $U(1)_A$ singlet quantity. In fact, it contains contributions carrying the $U(1)_A$ charge 2, 0 and -2. Thus χ is an appropriate quantity to observe the fate of the $U(1)_A$ symmetry even in the chiral symmetric phase, in principle, even though careful attention should be paid in order to infer correct meanings.

In this respect, the discussions of Schaffner-Bielich [15] is obscure; he discusses under the assumption that χ and the $U(1)_A$ anomaly are equivalent to each other and that the dropping of χ at T_c immediately means the effective restoration of the $U(1)_A$ symmetry. His assumption is considered as correct only if the dropping rate of χ is much faster than that of f_π . To judge the validity for this prevailing assumption is what we pursue in the present work. In fact, as discussed below, our result reveals that the assumption has no convincing reliability, at least, within the framework of the NJL model.

Now we consider the temperature dependence of χ in the NJL model. Among the four parameters (m_s, Λ, G, K), we might reasonably fix m_s and Λ at the values determined at zero temperature. In general, however, we should take account of temperature dependences of the coupling constants $G\Lambda^2$ and $K\Lambda^5$. As for $G\Lambda^2$, it would be hard or almost hopeless to get information about the temperature dependence even in some phenomenological sense.

Here, we make an assumption that $G\Lambda^2$ does not depend on temperature. This might be partially justified by the fact that even if $G\Lambda^2$ is constant, the NJL model restores the chiral symmetry as a consequence of its own dynamics.

We now pay attention to the behavior of $K\Lambda^5$, which indicates the temperature dependence of the $U(1)_A$ anomaly. For the first case, we treat $K\Lambda^5$ as a constant parameter and fix it at the values at zero temperature. We will call this prescription CASE A. The calculated temperature dependence of χ is shown in Fig. 3 (the solid line). We see that χ in the NJL model drops near T_c as the dynamical consequence and reproduces the lattice data up to $1.4T_c$ considerably well. This result means that the $U(1)_A$ symmetry is not restored at least up to $1.4T_c$, and we conclude that the effective restoration of the $U(1)_A$ symmetry does not coincide with the chiral phase transition.

At high temperatures, of course, we cannot judge whether or not the $U(1)_A$ symmetry is restored, since we lack the lattice data in those temperatures. If we believe that the instanton density is suppressed exponentially at high temperatures as is expected by the Pisarski-Yaffe factor [9], and the correlation of the topological charges, i.e., χ is also suppressed exponentially, the fitted line for the lattice data with a Fermi function in Fig. 3 (the dashed line) could be considered as reasonable behavior. We notice here the deviations of the NJL calculation (the solid line) from the fitted line at high temperatures. As the CASE B, we let $K\Lambda^5$ have the temperature dependence such that it reproduces the fitted line of χ . The calculated temperature dependence of $K\Lambda^5$ for this case is shown in Fig. 4.

We notice that there are two lumps around T_c . It would be senseless to take them seriously since we have ignored the temperature dependence of $G\Lambda^2$ that should have been taken into account in principle. Rather, we should note that the $U(1)_A$ symmetry is restored at high temperatures as is expected from the starting assumption that the instanton density is suppressed at those temperatures; the consistency is maintained in the NJL model.

We now calculate the constituent quark masses, the meson masses, and the pion decay constant in our CASE A and CASE B. The results are shown in Figs. 5~12. The qualitative features are almost the same as those of the CASE I by Hatsuda and Kunihiro [4].

Finally, we give the temperature dependence of $m_{\eta'}$ in Figs. 13 and 14 that could be obtained by utilizing the Witten-Veneziano mass formula (1). The η' mass goes to infinity at around $T_c = 200$ MeV in either CASE A or B. This is because f_π gets to zero at that temperature. We have removed those infinities above the temperature at which f_π vanishes because it is considered that our approximation scheme is broken down there.

IV. SUMMARY

We have derived the expression for the topological susceptibility, χ , in the NJL model within the same approximation as for the constituent quark masses and the meson masses, namely in the leading order of large N_c expansion. At zero temperature, we have performed parameter setting by employing χ in place of $m_{\eta'}$, and have seen that the obtained parameters do not allow the bound state of η' . At finite temperature, we have calculated the temperature dependence of χ , and have found that the lattice data up to $1.4T_c$ are reproduced with a constant six-point coupling constant K . This means that the $U(1)_A$ symmetry is not restored up to $1.4T_c$, and we are led to the conclusion that within the present framework, the effective restoration of the $U(1)_A$ symmetry and the chiral phase transition do not necessarily occur simultaneously even though the rapid dropping of χ around the chiral transition, observed in the lattice simulation, seemingly suggest the simultaneous restoration. At high temperatures, we cannot state anything definitely because of the absence of the lattice data. We have shown, however, that if χ is suppressed exponentially, the $U(1)_A$ symmetry is allowed to be restored at high temperatures.

The topological susceptibility is an interesting quantity because it is related to the mass of η' through the Witten-Veneziano mass formula. At zero temperature, we have seen that the formula is satisfied numerically in the NJL model. At finite temperature, by utilizing the formula, we have obtained knowledge as to the temperature dependence of $m_{\eta'}$. In NJL model, η' is far from a stable particle even if it exists. Therefore we would say that the parameter setting by using $m_{\eta'}$ is somewhat obscure. Our approach proposed in this article

is, on the other hand, not affected by questionable quantities such as $m_{\eta'}$ and as a result it takes the advantage to extract reliable results even when the bound state of η' cannot be available in the NJL model.

ACKNOWLEDGMENTS

We would like to thank T. Matsui, H. Fujii and M. Ohtani for precious and valuable comments. One of authors (K. F.) thanks L. von Smekal for the discussion about the interpretation of χ obtained here [17].

REFERENCES

- [1] E. Witten, Nucl. Phys. B **156**, 269 (1979)
- [2] G. Veneziano, Nucl. Phys. B **159**, 213 (1979)
- [3] S. P. Klevansky, Rev. Mod. Phys. **64**, 649 (1992)
- [4] T. Hatsuda and T. Kunihiro, Phys. Rep. **247**, 221 (1994)
- [5] U. Vogl and W. Weise, Prog. Part. Nucl. Phys. **27**, 195 (1991)
- [6] D. Lehmann, Ph.D. thesis, Erlangen-Nürnberg University, 1998
- [7] B. Allés, M. D’Elia, and A. Di Giacomo, Nucl. Phys. B **494**, 281 (1997)
- [8] M. Takizawa and M. Oka, Phys. Lett. B **359**, 210 (1995); erratum **364**, 249 (1995); M. Takizawa, Y. Nemoto, and M. Oka, Austral. J. Phys. **50**, 187 (1997); Phys. Rev. D **54**, 6777 (1996); Phys. Rev. D **55**, 4083 (1997)
- [9] E. Shuryak, Comments Nucl. Part. Phys. **21**, 235 (1994)
- [10] R. Alkofer, P. A. Amundsen and H. Reinhardt, Phys. Lett. B **218**, 75 (1989)
- [11] T. D. Cohen, Phys. Rev. D **54**, 1867 (1996); S. H. Lee and T. Hatsuda, Phys. Rev. D **54**, 1871 (1996),
- [12] C. Bernard *et al.*, Phys. Rev. Lett. **78**, 598 (1997)
- [13] S. Chandrasekharan, D. Chen, N. Christ, W. Lee, R. Mawhinney, and P. Vranas, Phys. Rev. Lett. **82**, 2463 (1999)
- [14] R. A. Janik, M. A. Nowak, G. Papp, and I. Zahed, hep-lat/9911024
- [15] J. Schaffner-Bielich, Phys. Rev. Lett. **84**, 3261 (2000)
- [16] M. Birse, T. Cohen and J. McGovern, Phys. Lett. B **388**, 137 (1996)
- [17] L. von Smekal, in private communications; he pointed out that the physical meaning

of χ_{NJL} is closer to χ_{full} rather than χ_{pure} . We are now making progress in our studies toward this direction.

FIGURES

FIG. 1. Three of various contracting ways are shown with their corresponding diagrams.

FIG. 2. Other leading order diagrams.

FIG. 3. The lattice data are plotted with error bars. We have fitted them with a Fermi function (the dashed line). The solid line denotes the result of the NJL model with constant $K\Lambda^5$.

FIG. 4. Temperature dependence of $K\Lambda^5$.

FIG. 5. The constituent quark masses for CASE A.

FIG. 6. The constituent quark masses for CASE B.

FIG. 7. The meson masses for CASE A.

FIG. 8. The meson masses for CASE B.

FIG. 9. The Kaon mass for CASE A.

FIG. 10. The Kaon mass for CASE B.

FIG. 11. The pion decay constant for CASE A.

FIG. 12. The pion decay constant for CASE B.

FIG. 13. The η' mass for CASE A.

FIG. 14. The η' mass for CASE B.

TABLES

	Hatsuda and Kunihiro [4]	Ours	Experimental/empirical values
m_u^* (MeV)	335	337	336
m_s^* (MeV)	527	523	540
m_η (MeV)	487	505	549
$m_{\eta'}$ (MeV)	(958)	None [942]	958
$\chi^{1/4}$ (MeV)	166	(175)	175
θ_η	-21°	-16.7°	-20°

TABLE I. Calculated physical quantities. Comparison of our results with Hatsuda-Kunihiro and experimental data. In parentheses are the values used as inputs. The value of $m_{\eta'}$ shown in the square brackets is inferred by the Witten-Veneziano mass formula.

FIG.1

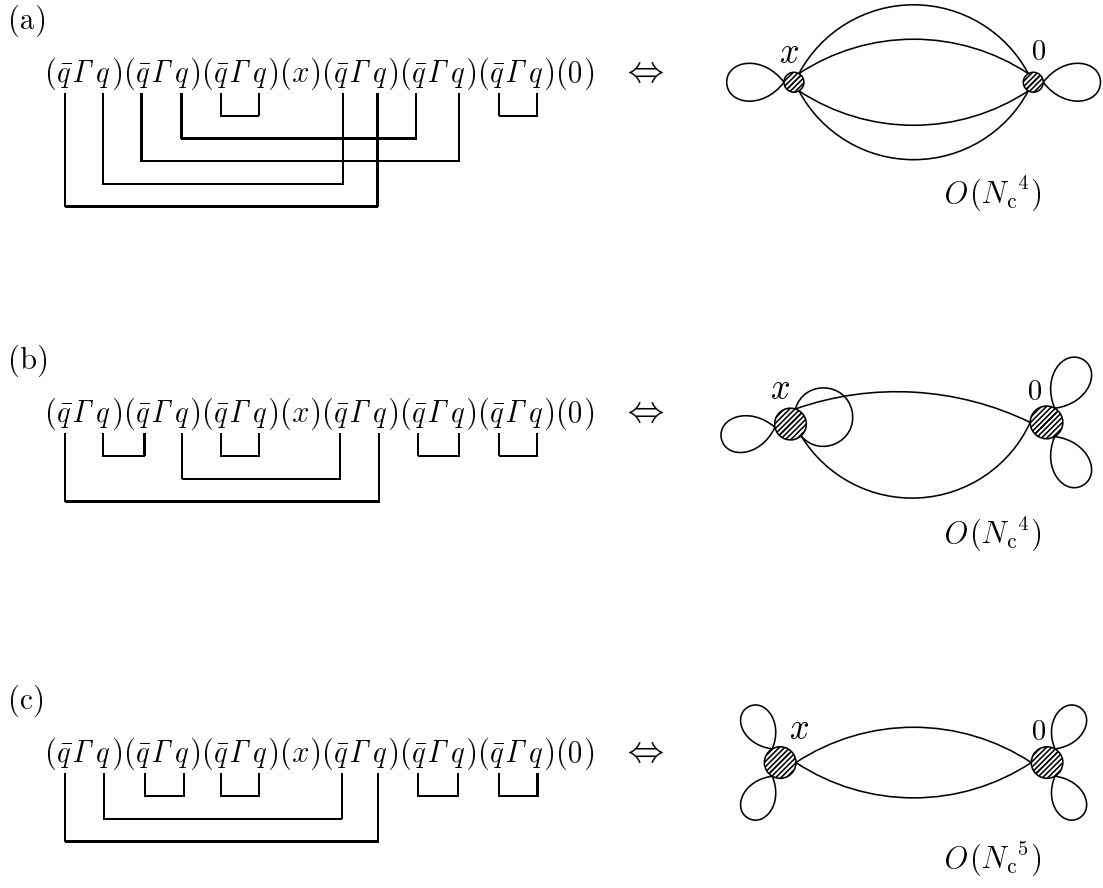


FIG.2

$$\chi^{(\text{ring})} = \begin{array}{c} \text{diagram 1} \\ \text{diagram 2} \\ \text{diagram 3} \end{array} + \dots$$

The diagram shows a series of three terms representing ring diagrams. Each term consists of two vertices, labeled d and i , connected by two arcs (one above and one below). Each vertex has two self-loops, labeled l and a . The first term has the self-loops l and a on vertex d . The second term has the self-loops l and a on vertex i . The third term has the self-loops l and a on both vertices d and i . The series is followed by an ellipsis $+\dots$.

FIG.3

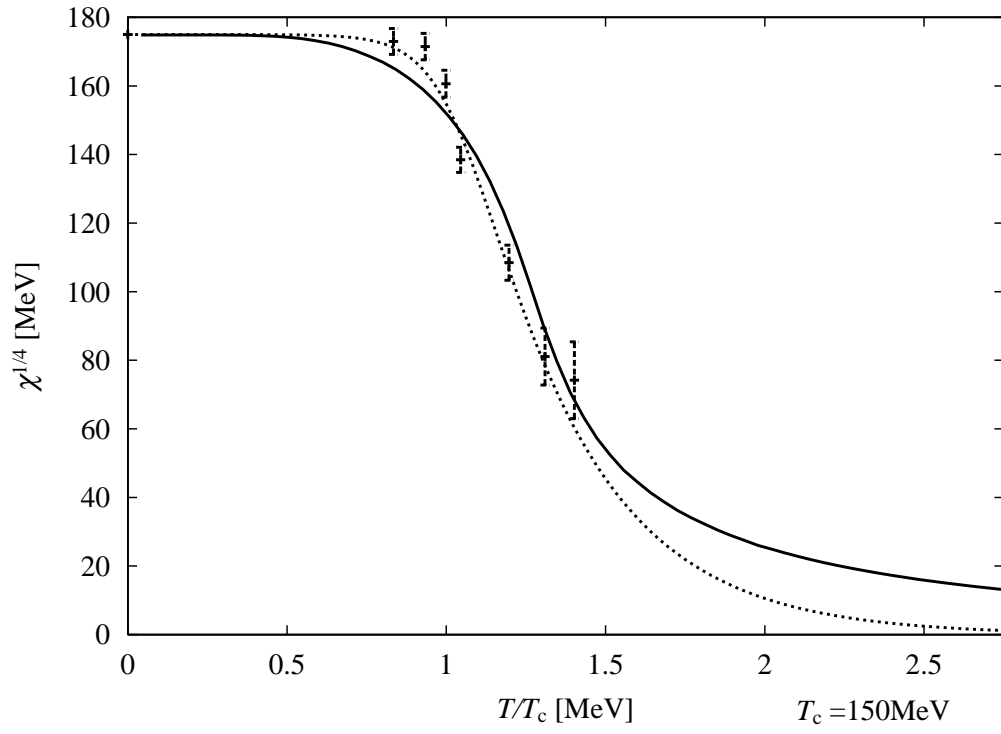


FIG.4

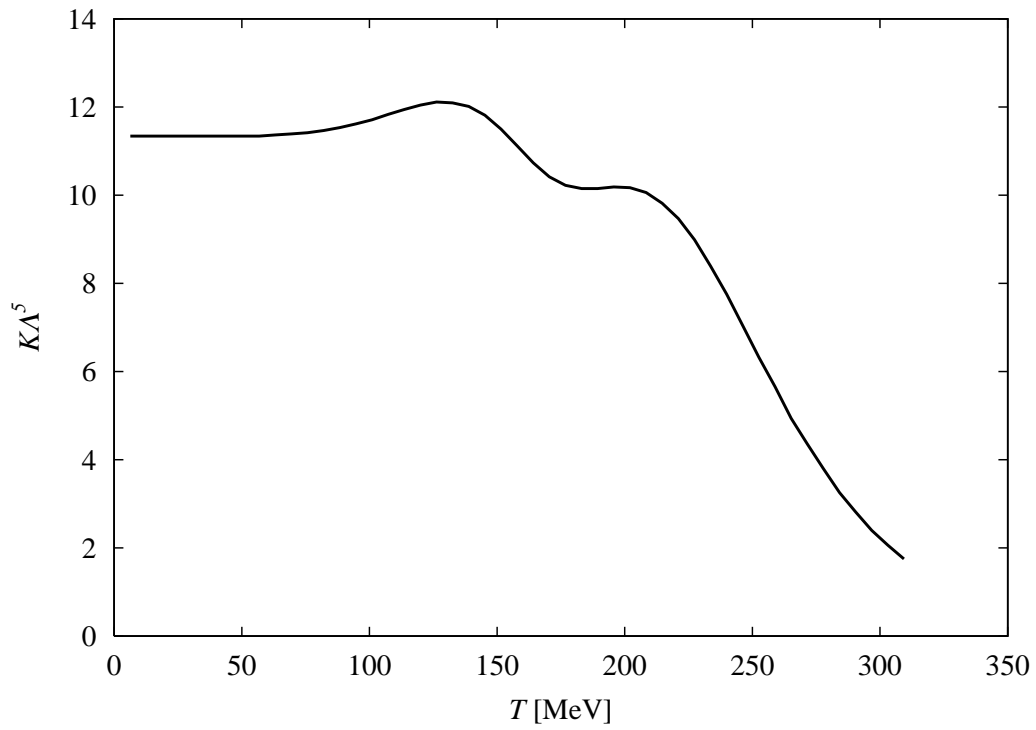


FIG.5

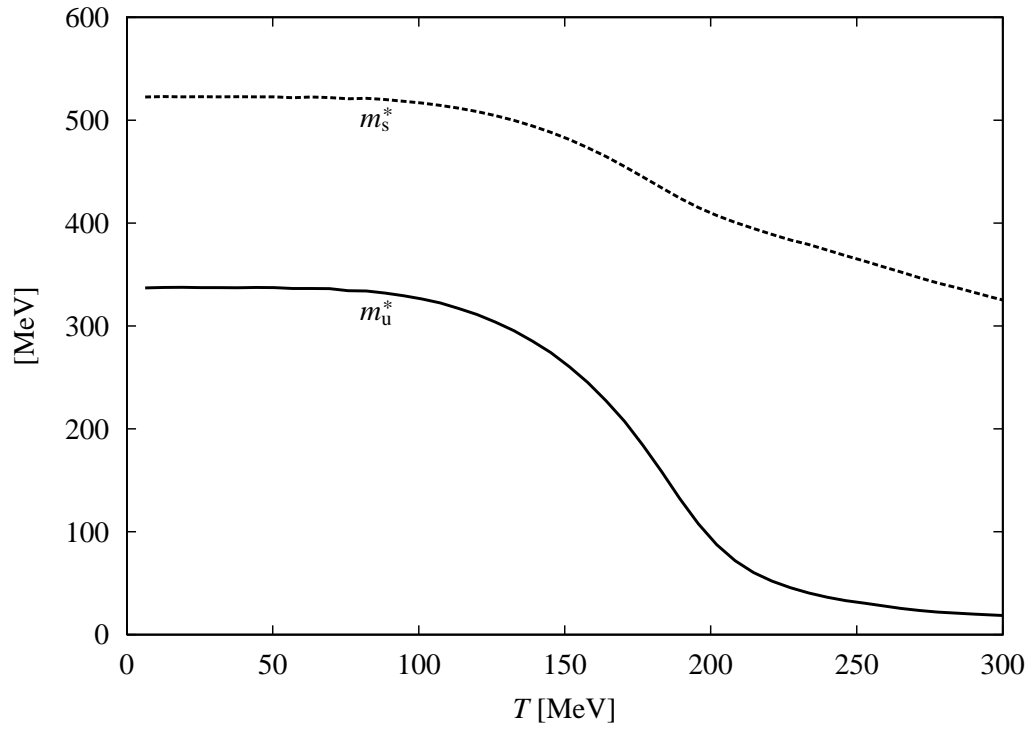


FIG.6

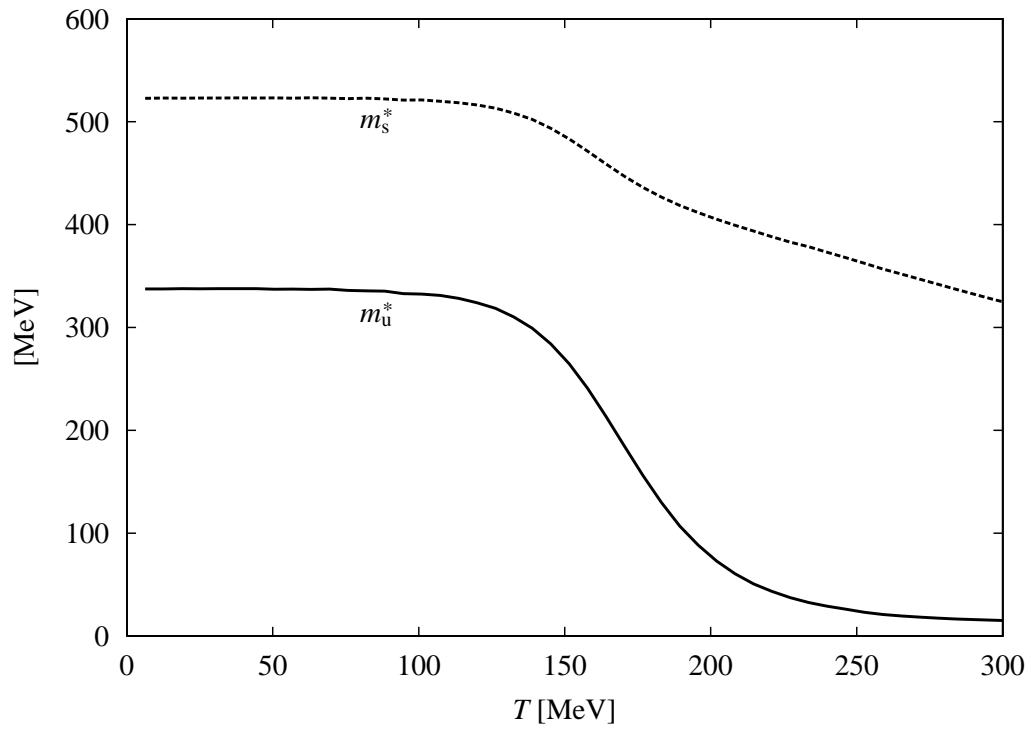


FIG.7

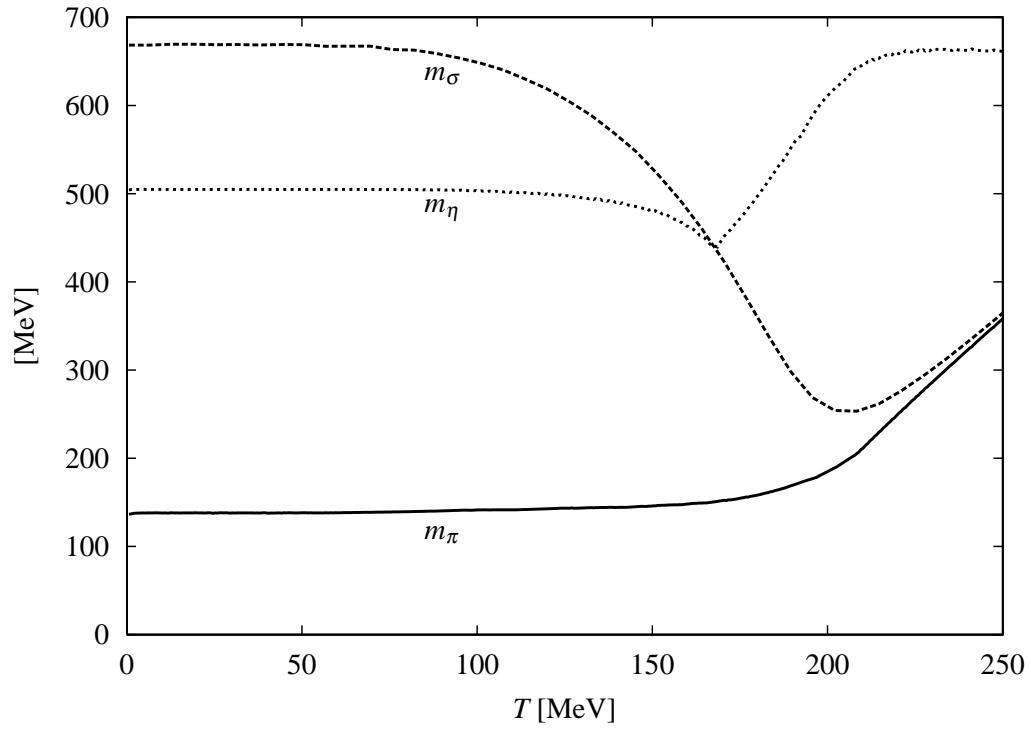


FIG.8

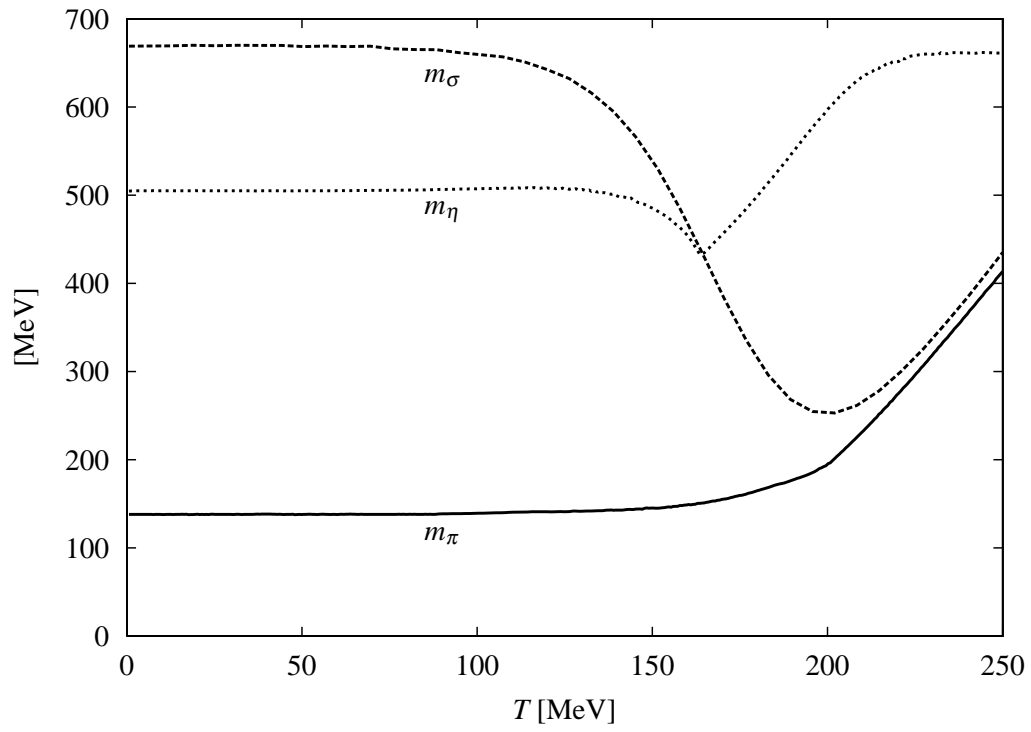


FIG.9

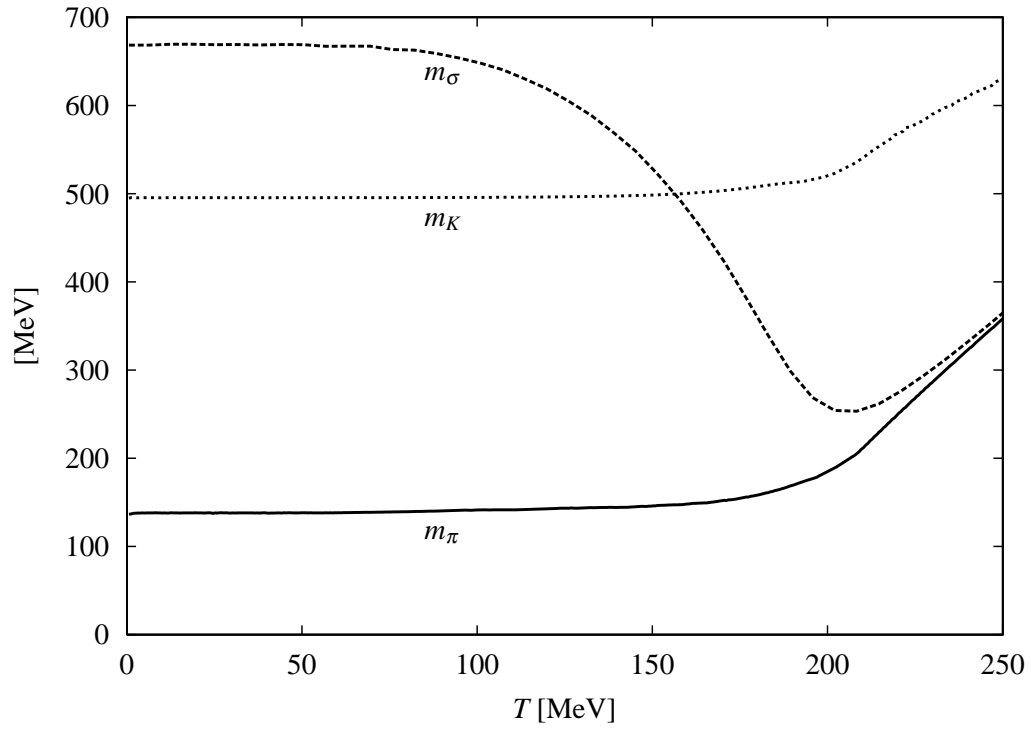


FIG.10

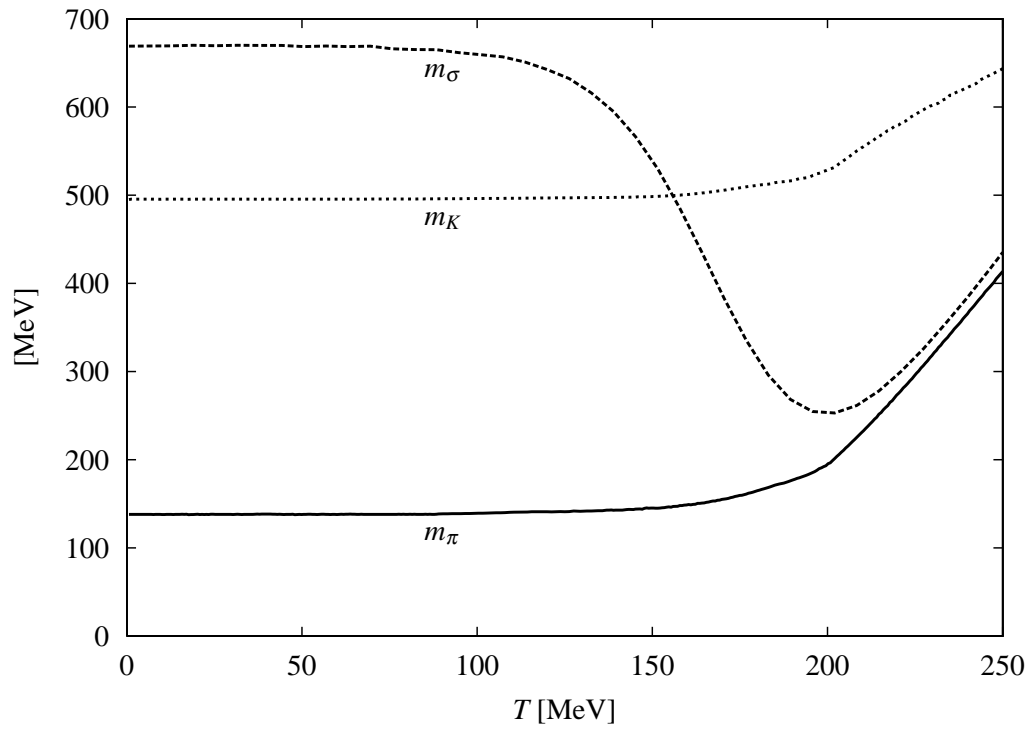


FIG.11

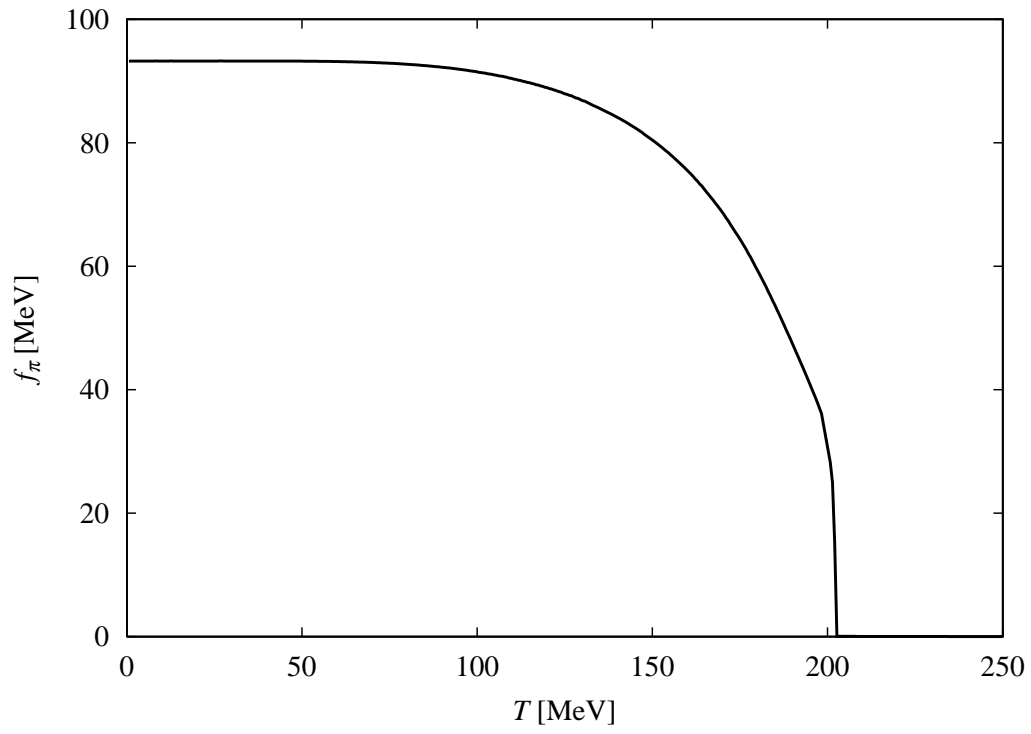


FIG.12

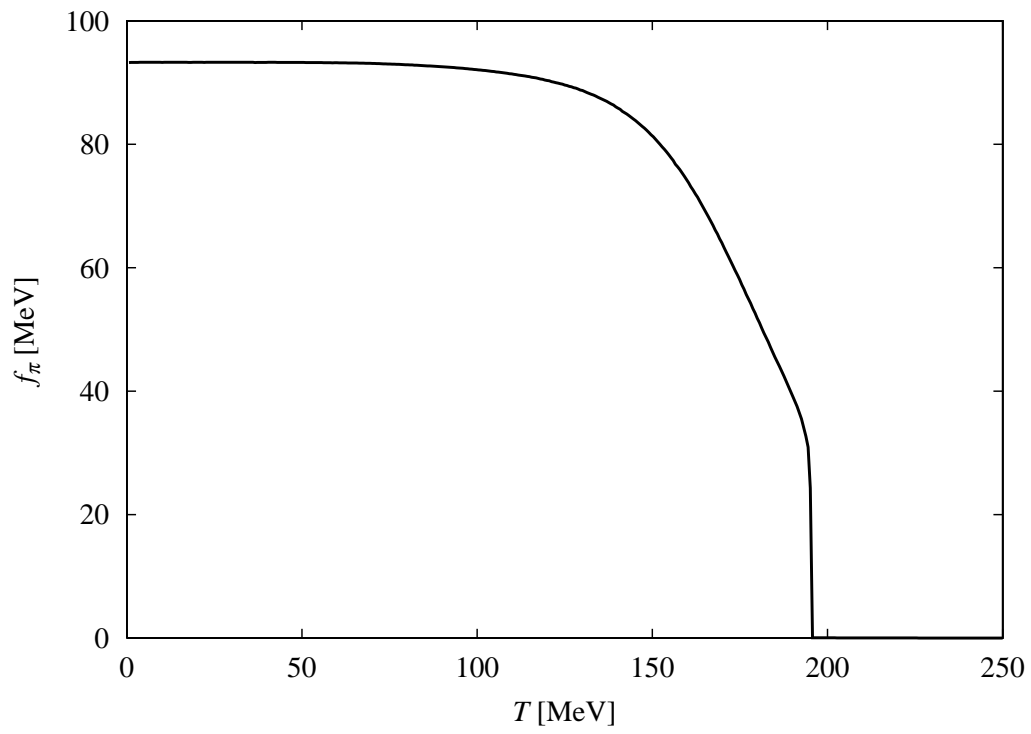


FIG.13

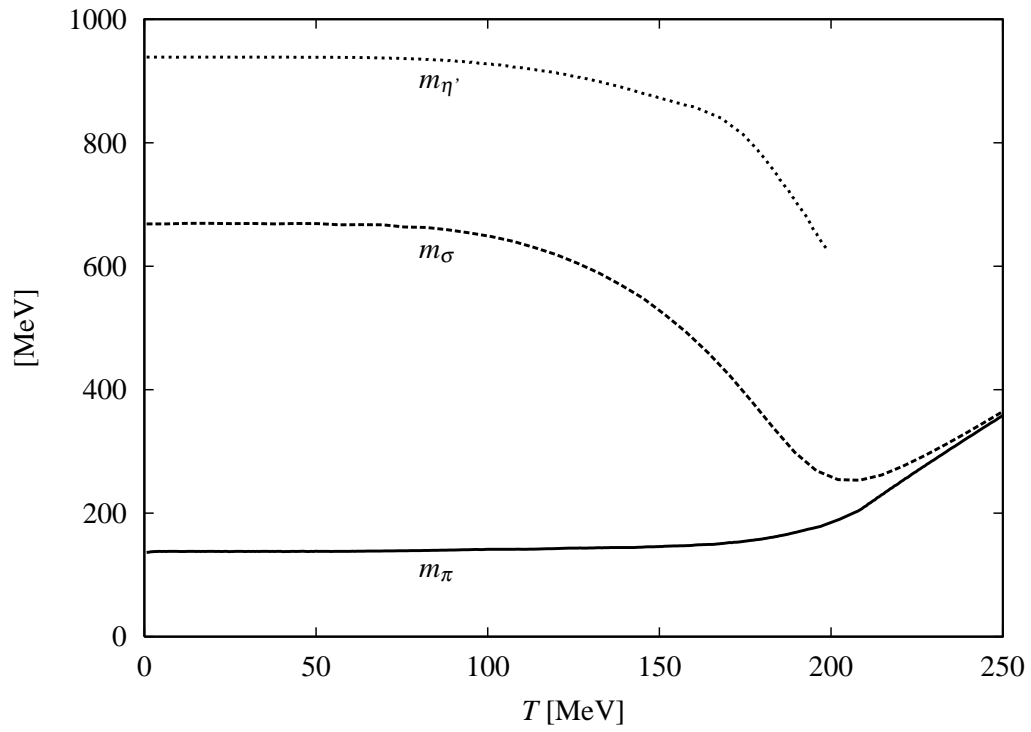


FIG.14

